

Birefringence in $\text{ZnP}_2\text{-D}_4^8$

Stamov I.G.

T.G. Shevchenko State University of Pridnestrovie
Tiraspol, Republic of Moldova

Zalamai V.V.

Institute of Applied Physics,
Academy of Sciences of Moldova,
Chisinau, Republic of Moldova

Nemerenco L., Syrbu N.N.
Technical University of Moldova
Chisinau, Republic of Moldova

Abstract — Spatial dispersion in $\text{ZnP}_2\text{-D}_4^8$ has been studied. The spectral dependences of the refractive index $n^c(E||c, k||a)$, $n^a(E||a, k||c)$ and $n^b(E||b, k||c)$ had been determined. $\text{ZnP}_2\text{-D}_4^8$ crystals are isotropic at $\lambda_0=612\text{nm}$ wavelength, in case of crossed polarizers a transmittance maximum is observed. It was shown that the dispersion is positive $n^c(E||c, k||a)$, $n^a(E||a, k||c) > n^b(E||b, k||c)$ in $\lambda > \lambda_0$ region, the dispersion is negative $n^c(E||c, k||a)$ at $\lambda < \lambda_0$, and $\Delta n = n^c - n^b = 0$ at $\lambda = \lambda_0$.

Keywords — Semiconductor compound; optical absorption and reflection spectra; optical constants; capacitance voltage characteristics; Schottky barrier; photodiodes

I. INTRODUCTION

Zinc diphosphide – is a wide gap semiconductor material of A^2B^5 group, which possesses the anisotropy of optical properties with natural gyrotropy [1 - 6]. Devices of quantum electronics and nonlinear optics had been elaborated basing on ZnP_2 crystals, which operating principle is based on gyrotropy and nonlinear crystal polarizability [7 - 12]. The values of nonlinear polarizability and gyrotropy of ZnP_2 are higher than those for other crystals [8, 13]. The low thermal conductivity of ZnP_2 crystals ($10 \text{ W/m} \cdot \text{K}$) is used to create laser beam deflectors with thermally induced gradient of the refractive index [9, 10]. It was shown the possibility of creating magneto-optical modulators basing on crystals of zinc and cadmium diphosphide, magneto-optical sensors for measuring the magnetic field [11, 13].

The technology for producing p-n junctions based on ZnP_2 crystals, surface barrier diodes was developed [2, 3, 5, 6]. The developed photoresists based on ZnP_2 possess a low relaxation time constant and are suitable for registering impulse radiation flows of 1·10⁻⁹s duration. Photoelectronic emitters and photodiodes, electric switches and Zener diodes had been developed based on ZnP_2 single crystals [14 - 17]. ZnP_2 crystals change the optical activity with temperature change, while maintaining the linear dependence of the rotational ability of polarization plane on the temperature (temperature sensors) [15, 16].

II. EXPERIMENTAL METHODS

The process of growing single crystals of zinc diphosphide from Zn and P precursors occurred in two stages. The first step was the synthesis conducted in a quartz ampoule placed in a pressure container ($\approx 40 \text{ atm.}$). 300-500 grams of

substance were synthesized simultaneously. The synthesized compound is sublimed in vacuum to obtain single crystals in the second step. The maximum dimensions of ZnP_2 ingots obtained from the gas phase reached $10 \times 10 \times 20 \text{ mm}$. The single crystals had been cleaved perpendicular to the C axis. The measurements were carried out on single crystals obtained in plates form or prisms grown along the C axis and having a not treated mirror surface. Schottky diodes, p-n junctions had also been obtained on the cleaved not polished surface. Optical transmission spectra in crossed polarizers were measured with MDR-2 and JASCO-670 spectrometers. Low-temperature measurements were made using LTS-32C330 Workhorse-type optical cryostat.

III. EXPERIMENTAL RESULTS AND DISCUSSIONS

A characteristic feature of $\text{ZnP}_2\text{-D}_4^8$ crystals is the dispersion of the refractive indices n_0 and n_e at the absorption edge (birefringence), which is associated with the peculiarities of the band structure. The selection rules of electronic transitions determine the nature (allowed, prohibited) of these electronic transitions. This will determine the value of absorption and dielectric constant in the respective polarizations, and hence the sign of birefringence. These features lead to the rapid growth of one of the refractive indices as approaching to the fundamental absorption edge. This determines the anisotropy of the interband absorption edge of the crystal in the respective polarizations. The intersection of the dispersion curves (isotropic point - IP) from the long wavelength side of the absorption edge is observed in ZnP_2 crystals.

The absorption is small and it is determined by several mechanisms in the region of transparency of the crystal – by natural optical activity or local polarized absorption bands of the impurities, defects, etc. The existence of two types of waves in the crystal – ordinary and extraordinary, for which there are two refractive indices n_0 and n_e , is determined by the crystal's dielectric tensor $\epsilon(\omega, k)$, which depends on the frequency ω , and the wave vector k . The spatial dispersion, i.e. the dependence of the dielectric constant on the wave vector k , causes the appearance of non diagonal element ϵ_{zz} of the tensor's dielectric permittivity. Thus, the refractive index $n_0 > n_e$ in the absorption edge and $n_0 < n_e$ in the transparency region. There is also an inverse relationship.

Mutually perpendicular light waves with refractive indices n_0 and n_e can interfere in the crystal.

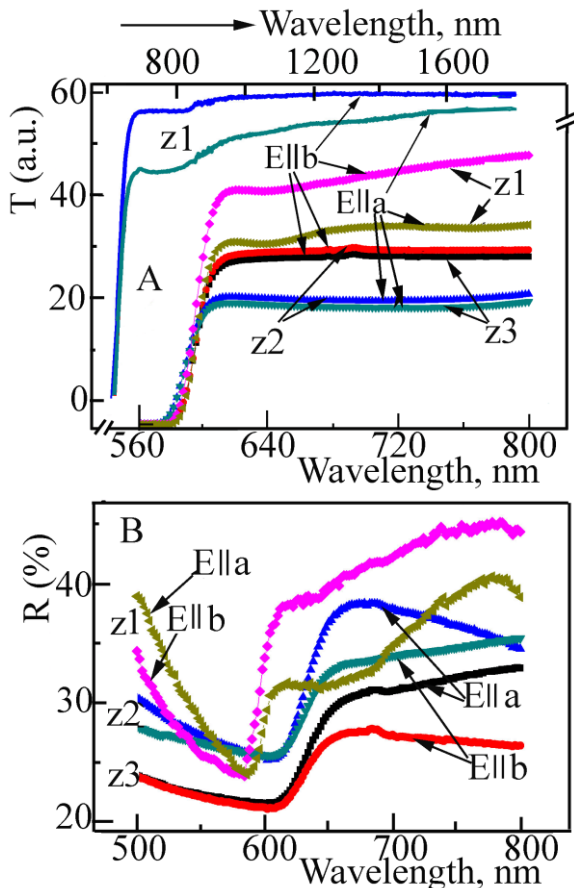


Fig. 1 A – Transmittance spectra of ZnP2-D48 crystals at E||a and E||b polarizations for undoped samples (z1) and antimony-doped 1% (z2) and 1,5% (z3), B- reflectivity spectra of the same samples in the beginning of the absorption edge.

The edge absorption is also polarized, and it is due to direct allowed transitions in the region of high absorption coefficients. The energy range E_g is 2.403 eV at E \perp c polarization, and is 2.445 eV at E||c polarization. These data indicate that the band gap at E \perp c polarization is less than at E||c polarization. The zones' splitting value is 42 meV at 9K [2, 3].

The transmittance spectra of ZnP2-D48 crystals are measured at room temperature in the E||a and E||b polarizations for undoped samples (z1) in the 560-1800nm region, fig. 1, A. The crystals had approximately the same thickness ($d = 245 \pm 5 \mu\text{m}$) and natural chipped surfaces. The value of the transmittance coefficient for the E||b polarization is a bit more than for the E||a polarization and in undoped crystals (z1) and antimony-doped 1% (z2) and 1.5% (z3), fig. 1, A. The reflection spectra in the beginning of the edge absorption for these samples are shown in fig. 1, B. It is clearly evident from the reflection spectra that the growth of the reflection coefficient for undoped samples (z1) starts at shorter wavelengths. The spectral dependence of the refractive indices for E||a, E||b and E||c (z1) polarizations and for the E||a

and E||b polarizations in samples doped with antimony 1% (z2) and 1.5% (z3) are calculated from the reflectance spectra using the Kramers-Kronig method, fig. 2.

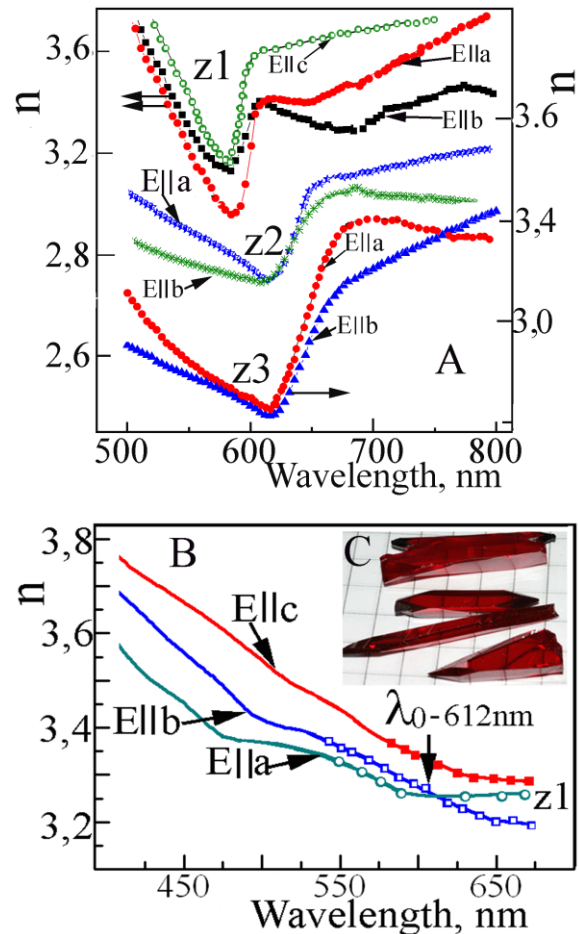


Fig. 2 A, B - The spectral dependences of the refractive index obtained from the Kramers - Kronig calculations for the E||c, k||a, E||a, k||c and E||b, k||c polarizations for undoped crystals (z1) and Sb-doped 1% (z2), 1.5% (z3); C - photos of ZnP2-D48 crystals.

The refractive indices of undoped crystals (z1) at E||a, k||c, E||b, k||c and E||c polarizations change almost in parallel and are increasing from $\lambda \approx 590$ nm with wavelength decrease. The refractive indices for all polarization grow with wavelength increase and the spectral dependence for E||a, k||c, E||b, k||c intersect in the wavelength range 600-615 nm, fig. 2. The spectral dependence of the refractive indices for all polarizations has higher values at wavelengths range $\lambda > 600$ -650 nm because the intensity of the reflected light from the crystal's back surface affects the reflection spectra. The spectral dependences of the refractive indices are determined from the interference spectra in the wavelength range $\lambda > 600$ nm at E||c, k||a, E||a, k||c, E||b, k||c polarizations, and jointed with the data from Kramers- Kronig calculation at $\lambda < 550$ nm for undoped crystals (z1), fig. 2, B. The spectral characteristics of the refractive indices are intersecting at 612 nm wavelength (λ_0) for the undoped samples. This wavelength is the isotropic wavelength of ZnP2 crystals.

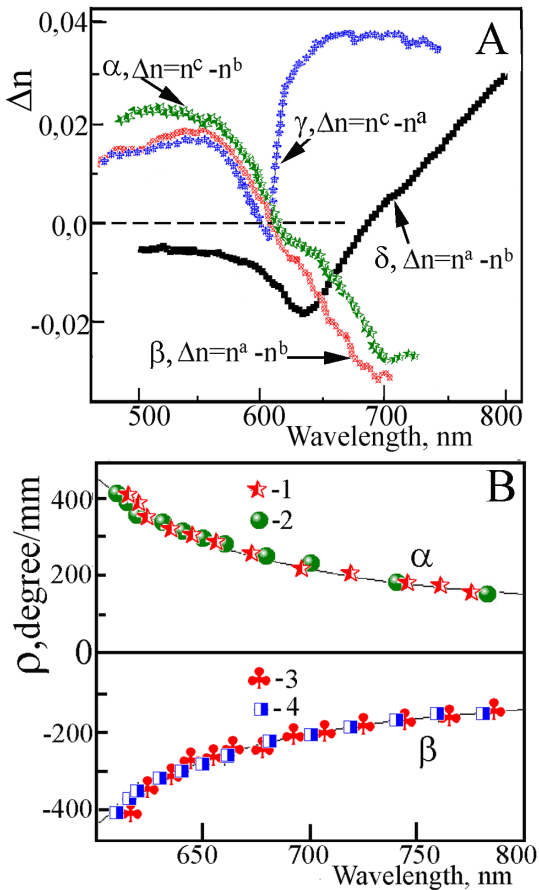


Fig. 3 A - The spectral dependence of the refractive index difference $\Delta n=n_a-n_b$, $\Delta n=n_c-n_a$ and $\Delta n=n_c-n_b$ of ZnP2 crystals, where n_a, n_b, n_c refractive indices for E||a, E||b, E||c polarizations, respectively (α, β, γ -undoped crystals, δ -doped crystals 1.5% Sb), B - the spectral characteristics of the rotation capacity of four undoped ZnP2 crystals, obtained under different processing conditions.

The spectral dependences of the difference of refractive indices $\Delta n=n_a-n_b$, $\Delta n=n_c-n_a$, $\Delta n=n_c-n_b$ in ZnP2 crystals are presented in fig. 3, A, where n_a, n_b, n_c are the refractive indices for E||a, E||b, E||c polarizations, respectively. The curves α and β correspond to the undoped crystals (z1), which include the correction of the interference spectra in the long wavelength region. The spectra are represented by curves γ and δ and the long wavelength region is not corrected with the data from the interference spectra. The α, β and γ spectra correspond to z1 crystals, and the δ spectra correspond to z3 crystals. The spectral dependence of the difference of refractive indices α is positive in the short-wavelength region $\lambda < \lambda_0$ (612nm), and in the long-wavelength region $\lambda > \lambda_0$ (612nm) has a negative value. This pattern confirms that the refractive indices are intersecting at 612nm wavelength for the E||a and E||b polarizations. Transmittance maximum is observed at this wavelength in the crystals' transmission spectra placed between crossed polarizers (fig. 3, A). λ_0 wavelength is shifted to shorter wavelengths region in accordance with the temperature coefficient of the offset absorption edges at E⊥c и E||c polarizations and 9 K. The difference of refractive indices difference $\Delta n=n_a-n_b$, $\Delta n=n_c-$

n_a , $\Delta n=n_c-n_b$ are positive values in the short-wavelength region of λ_0 . These values for the difference of the refractive indices are negative in the long-wavelength region of λ_0 , fig. 3, A. This crystal is a phase plate in which two light waves propagate at different speeds.

Rotation of the polarization plane of light waves is observed in case of the propagation of light waves along the C axis of ZnP2 crystals. ZnP2 -D48 crystals possess a natural optical activity. The optical activity is observed along the C axis of the uniaxial ZnP2 -D48 crystal. It is not active on the perpendicular orientation to the optical axis C. The crystal has a linear birefringence along these directions. The studies of rotatory ability of ZnP2 crystals had been made on plates of different thickness (from 50 μm up to 1 mm). The samples were prepared by cleaving the crystals' cleavage plane (001).

Fig. 3, B shows the dispersion curves of the rotation ability for undoped ZnP2 crystals, obtained under different processing conditions. The value of the rotation ability for left and right rotating planes of light's polarization increases near the fundamental absorption edge. The characteristics of the optical activity are practically identical in the left and right rotating ZnP2 crystals, obtained in different technological regimes (fig. 3, B).

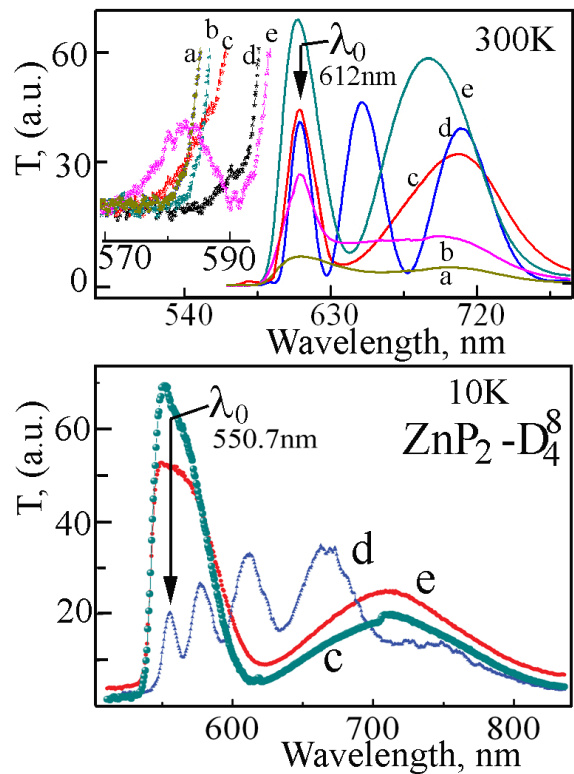


Fig. 4 The transmittance spectra (T) of ZnP2 -D48 crystals with 18.7 μm (a), 45 μm (b), 179 μm (c), 270 μm (d) 1450 μm (e) thickness in the crossed polarizers at 300 K (top) and 10 K (bottom).

The spectral dependence of the transmittance coefficient T of -D48 crystal placed between crossed polarizers is shown in fig. 4. Transmittance maxima at different wavelengths are detected in transmittance coefficient of crystals with 18.7 μm (a), 45 μm (b), 179 μm (c), 270 μm (d) 1450 μm (e) thickness

in crossed polarizers at 300 K and 10 K. When the thickness of the crystals change from 18.7 μm to 1450 μm the maximum practically does not change its position at a wavelength of 612 nm (300K) and 550.7 nm (10K). The wavelength of 612 nm (300 K) for ZnP2 crystals is the isotropic wavelength - λ_0 , at this wavelength, the crystal does not distinguish the polarization of light waves. Such a wavelength of 550.7 nm is detected at 10K. When the thickness of the crystals changes on the long-and short-wavelength region of λ_0 there are appearing additional peaks.

Minima (maxima) of interference pattern closest to the passband shift toward each other with increasing thickness of the crystal and merge into one minimum (maximum) localized at a λ_0 wavelength for the crystal thickness $d \sim 10\text{mm}$. The interference pattern is due to the fact that when you remove the wavelength of λ_0 , there is a linear birefringence and the optical activity appears as an elliptical birefringence. The phase difference between two elliptically polarized components acquired on a single path is (1):

$$\Delta\varphi = \frac{2\pi}{\lambda} \left[(\Delta n)^2 + \left(\frac{g_{11}}{n} \right)^2 \right]^{1/2}, \quad (1)$$

where $\Delta n = n_e - n_o$ - ZnP2-D48 crystal's birefringence, λ - wavelength, g_{11} - nonzero component of the gyration tensor of light propagation along the [001] direction of ZnP2 -D48 crystal, n - average refractive index. As a result, a linearly polarized light passing through the crystal is elliptically polarized. The orientation of the ellipse relative to the optical axis of the crystal and the ellipticity depend on the conditions of the incident light wavelength. The intensity changing of light passing between crossed polarizers out of the spectral region λ_0 is described by the expression, which is derived from a consideration of the interference phenomena, taking into account the crystal's gyrotropy:

$$I = I_0 \rho^2 \frac{\sin^2 \left\{ \left[\rho^2 + \left(\frac{\pi \Delta n}{\lambda} \right)^2 \right]^{1/2} \right\}}{\rho^2 + \left(\frac{\pi \Delta n}{\lambda} \right)^2}, \quad (2)$$

where ρ - the value of the specific rotation of the crystal. When $\Delta n = 0$, the expression (2) is transformed into a simpler form. Maxima of interference pattern take place in the condition:

$$\left[\rho^2 + \left(\frac{\pi \Delta n}{\lambda} \right)^2 \right]^{1/2} d = \left(m + \frac{1}{2} \right) \pi, \quad m = 0, 1, 2, \dots, \quad (3)$$

and minima in the condition:

$$\left[\rho^2 + \left(\frac{\pi \Delta n}{\lambda} \right)^2 \right]^{1/2} d = m\pi, \quad m = 0, 1, 2, \dots \quad (4)$$

Expressions (3) and (4) show that the spectral position of the maxima and minima is observed on both sides of the abnormal passband if changing the crystal's thickness. The interference pattern is changed so that the side lobes maxima are shifted towards each other and have a low intensity at a certain thickness.

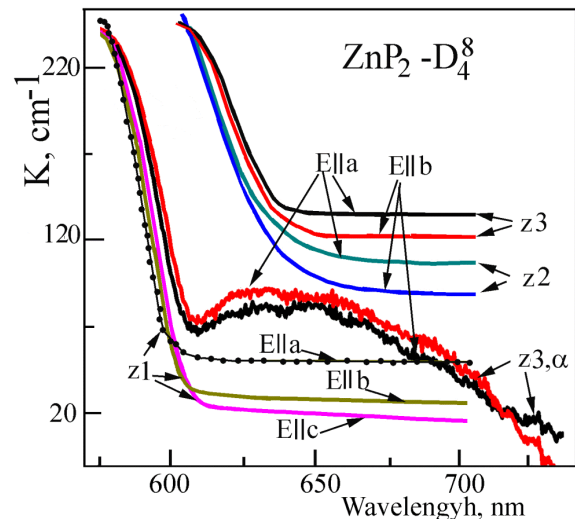


Fig. 5 The absorption spectra of undoped ZnP2 crystals at E||a, E||b, and E||c polarizations and of Sb-doped crystals 1%, Sb(z2) and 1.5%, Sb(z3), α curves were measured at 10 K.

Reflection spectra in the region of the beginning of edge absorption and the calculated values of the refractive indices (CC) show that the beginning of edge absorption of Sb-doped crystals is shifted to longer wavelengths, fig. 1, B, fig. 2, A and fig. 3, A. This is clearly seen in the reflection spectra (fig. 1, A) and in the spectral dependence of the refractive index (fig. 2, A) and in the difference between them (fig. 3, A). The starting of the beginning of edge absorption of Sb-doped crystals is particularly evident in case of low temperatures, [19]. At 10 K temperature the spectral dependences of light absorption coefficient are almost identical near their isotropic wavelength $\lambda_0 \approx 550.7$ nm at E||c and E \perp c polarizations, but at E||c polarization the absorption coefficient is greater ($\approx 12 \text{ cm}^{-1}$) than at E \perp c polarization, [19].

Absorption spectra of undoped ZnP2 crystals at E||a, E||b, and E||c polarizations and Sb-doped crystals (1%) (z2), and Sb-doped (1.5%) (z3), are presented in fig. 5. The spectra shown with the curves z3, α , are measured at 10 K. The difference in the absorption coefficients is observed for the E||a and E||b polarizations at all crystals. This difference is somewhat larger ($\approx 25 \text{ cm}^{-1}$) for the undoped crystals (z1) than for the doped crystal (z2, z3 $\approx 15 \text{ cm}^{-1}$). The edge absorption of z2, z3 crystals starts to increase rapidly at 640nm wavelengths and for undoped z1 crystals a sharp increase in the absorption begins at 600 nm wavelengths, fig. 5. Broad absorption band near the beginning of the edge absorption is released at a 10 K temperature in the spectra of crystals doped with antimony, fig. 5, curves z3, α . The beginning of edge absorption is shifted to shorter wavelengths at 10 K.

IV. CONCLUSIONS

The spectral dependences of the refractive indices n_c (E||c, k||a), n_a (E||a, k||c) and n_b (E||b, k||c) in ZnP2-D48 crystals which are determined from the interference, transmittance and reflectance spectra using the Kramers-Kronig method intersect at a wavelength $\lambda_0 = 612$ nm. The crystals are isotropic at a λ_0 wavelength and in case of crossed polarizers have a

maximum bandwidth. The of refractive indices $n_c(E||c, k||a)$ and $n_a(E||a, k||c)$ are higher in the λ_0 wavelength region, than the refractive indices at $n_b(E||b, k||c)$ polarization, the dispersion is positive. Inverse relationship was observed in the long-wavelength region, the dispersion is negative. $\Delta n = n_c - n_b = 0$ at $\lambda_0 = 612$ nm wavelength. Such crystal represent a phase plate in which two light waves propagate with the speeds $V_x = c/n_k||c$ and $V_y = c/n_k||a$.

REFERENCES

- [1] V.B. Lazarev, V.J. Sevcenco, J.H. Grinberg, V.V. Sobolev, Poluprovodnicovye soedineniia grupy A^{II} B^V, Nauca, Moseva, 1978.
- [2] N.N. Syrбу, Optoelectronic Properties of II–V Compounds, Stiinta, Kishinev 1983.
- [3] N.N. Syrбу, I.G. Stamoв, A.I. Kamertsel, Sov. Phys. Semicond. 26, 7 (1992) 665, Original Russian Text published in Fizica i Tehnica Poluprovodnikov, 26 (1992), pp. 1191-1224.
- [4] I.V. Bodnari, M.A. Osipova, V.Yu. Rud, Yu.V. Rud, B.Kh. Bairamov, Journal of Applied Spectroscopy, Vol.77, No.1 (2010), pp.146-151.
- [5] N.N. Syrбу, A.I. Kamertsel, I.G. Stamoв, Sov. Phys. Semicond. 24, 4 (1992) 376, Original Russian Text published in “Fizica i Tehnica Poluprovodnikov”, 26 (1992) pp. 666-678.
- [6] I.G. Stamoв, D.V. Tkacenco, Semiconductors, 2008, Vol.42, No.6, pp. 662, Original Russian Text, published in “Fizica i Tehnica Poluprovodnikov”, 2008, Vol.42, No.6, pp. 679-685.
- [7] I.I. Patscun, I.A. Sliukhina, Semiconductor Physics, Quantum Electronics and Optoelectronics, V.7, No.1 (2005), p. 31-35.
- [8] V.M. Trukhan, A.U. Sheleg, I.F. Fekeshgazi, “Photoelectronics”, No.13, (2004) 200.
- [9] V.A. Zuev, V.G. Fedotov, A.G. Bychkov, E.M. Smolearenko, V.M. Truhan, V.N. Yakimovich “Quantum electronics” 1988, 34.
- [10] V.M. Trukhan, A.U. Sheleg, and all. Patent Belarus №12388, 30.10.2009.
- [11] V.M. Trukhan, L.E. Soshnikov, S.E. Marenkin, T.V. Haliakevich, Inorganic Materials, Vol. 41, No.9 (2005), pp. 901-905., Translated from Neorganicheskie Materialy, Vol.41, No.9 (2005), pp. 1031-1036.
- [12] A.U. Sheleg, A.A. Kutas, V.N. Iakimovic, V.G. Fedotov, D.N. Karlikov, L.M. Gorynia, Patent SU, №875959 22.06.1981.
- [13] V.A. Gnatyuk, V.V. Borshch, M.G. Kuzmenko, O.S. Gorodnychenko, S.O. Yuryev, Physics and Chemistry of Solid State, V.5, No.2 (2004), p. 256-259.
- [14] N.N. Syrбу, I.G. Stamoв, A.G. Umanetc, Patent SU, №816345, 21.11.1980, Patent SU, №865040, 14.05.1981.
- [15] A.A. Andreev, B.T. Meleh, V.M. Truhan, Patent SU, №621254, 27.04.1978.
- [16] V.P. Novikov, A.U. Sheleg, V.M. Truhan, V.G. Fedotov, A.G. Bychkov, D.N. Karlikov, L.M. Gorynea, Patent SU, № 917004, 01.12.1981.
- [17] V.Yu. Rudi, Yu.V. Rudi, I.V. Bodnari, Jurnal techniceskoi fizici, 80 (2010), 84.
- [18] I.G. Stamoв, N.N. Syrбу, A.V. Dorogan, Physica B 412(2013) 130.
- [19] I.G. Stamoв, N.N. Syrбу, V.V. Zalamai, Journal of Luminescence, 149, (2014), 19.